

POLAR CONVECTION MONITORING DETERMINATION OF THE IMF BZ AND BY ORIENTATIONS FROM DIGISONDE DRIFT VELOCITIES

**J. L. Scali
B. W. Reinisch
C. G. Dozois**

**University of Massachusetts, Lowell
Center for Atmospheric Research
450 Aiken Street
Lowell, MA 01854**

August 1995

Scientific Report No. 9

APPROVED FOR PUBLIC RELEASE; DISTRIBUTION UNLIMITED

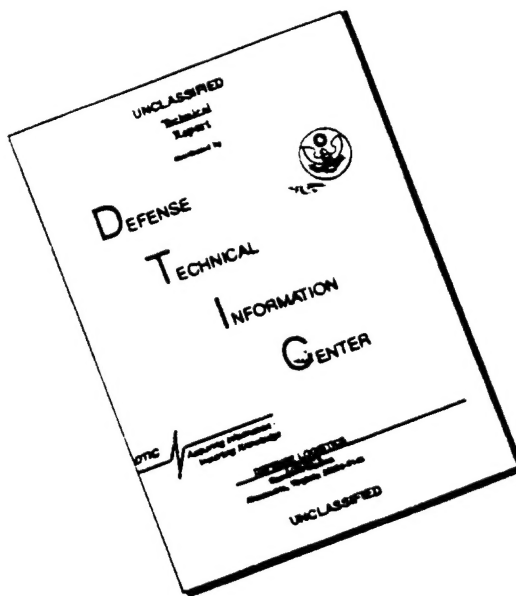


**PHILLIPS LABORATORY
Directorate of Geophysics
AIR FORCE MATERIEL COMMAND
HANSCOM AFB, MA 01731-3010**

19960319 090

DATA RELEASED 2024-01-26 14:00:00

DISCLAIMER NOTICE



THIS DOCUMENT IS BEST
QUALITY AVAILABLE. THE COPY
FURNISHED TO DTIC CONTAINED
A SIGNIFICANT NUMBER OF
PAGES WHICH DO NOT
REPRODUCE LEGIBLY.

"This technical report has been reviewed and is approved for publication."

B. S. Dandekar

BALKRISHNA S. DANDEKAR
Contract Manager

Edward J. Berghorn

Maj EDWARD BERGHORN, Chief
Ionospheric Application Branch

William K. Vickery

WILLIAM K. VICKERY, Director
Ionospheric Effects Division

This report has been reviewed by the ESC Public Affairs Office (PA) and is releasable to the National Technical Information Service (NTIS).

Qualified requestors may obtain additional copies from the Defense Technical Information Center (DTIC). All others should apply to the National Technical Information Service (NTIS).

If your address has changed, or if you wish to be removed from the mailing list, or if the addressee is no longer employed by your organization, please notify PL/TSI, 29 Randolph Road, Hanscom AFB, MA 01731-3010. This will assist us in maintaining a current mailing list.

Do not return copies of this report unless contractual obligations or notices on a specific document requires that it be returned.

REPORT DOCUMENTATION PAGE

Form Approved
OMB No. 0704-0188

Public reporting burden for this collection of information is estimated to average 1 hour per response, including the time for reviewing instructions, searching existing data sources, gathering and maintaining the data needed, and completing and reviewing the collection of information. Send comments regarding this burden estimate or any other aspect of this collection of information, including suggestions for reducing this burden, to Washington Headquarters Services, Directorate for Information Operations and Reports, 1215 Jefferson Davis Highway, Suite 1204, Arlington, VA 22202-4302, and to the Office of Management and Budget, Paperwork Reduction Project (0704-0188), Washington, DC 20503.

1. AGENCY USE ONLY (Leave blank)	2. REPORT DATE	3. REPORT TYPE AND DATES COVERED	
	August 1995	Scientific No. 9	
4. TITLE AND SUBTITLE		5. FUNDING NUMBERS	
Polar Convection Monitoring Determination of the IMF Bz and By Orientations From Digisonde Drift Velocities		PE12417F PRESDO TA 01 WUAB F19628-90-K-0029	
6. AUTHOR(S)		8. PERFORMING ORGANIZATION REPORT NUMBER	
J. L. Scali B. W. Reinisch C. G. Dozois			
7. PERFORMING ORGANIZATION NAME(S) AND ADDRESS(ES)		10. SPONSORING / MONITORING AGENCY REPORT NUMBER	
University of Massachusetts, Lowell Center for Atmospheric Research 450 Aiken Street Lowell, MA 01854		PL-TR-95-2138	
9. SPONSORING / MONITORING AGENCY NAME(S) AND ADDRESS(ES)		11. SUPPLEMENTARY NOTES	
Phillips Laboratory 29 Randolph Road Hanscom AFB, MA 01731-3010			
Contract Manager: B. S. Dandekar/GPIA			
12a. DISTRIBUTION / AVAILABILITY STATEMENT		12b. DISTRIBUTION CODE	
Approved for Public release, distribution unlimited			
13. ABSTRACT (Maximum 200 words)			
<p>Statistics for one year of Digisonde drift velocities recorded at Qaanaaq (Greenland) are used to derive a method to determine the sign of the interplanetary magnetic field Bz and By components. The Digisonde velocities show characteristics expected from the theoretical understanding of the two-cell and four-cell convection pattern which can exist at high latitudes when the IMF Bz < 0 and Bz > 0 respectively. The derived method is able to determine correctly the orientation of the IMF in 60 to 70% of the cases tested. Considering that the method uses only 15 minute drift velocities recorded at one station (Qaanaaq), the method shows enormous potential for accurately determining the orientation of the IMF components, and assisting in the mapping of the convection pattern when more data from Digisonde stations are introduced in the analysis.</p>			
14. SUBJECT TERMS		15. NUMBER OF PAGES	
Polar Convection Monitoring two-cell and four-cell convection patterns interplanetary magnetic field, Digisonde Drift Velocities		30	
		16. PRICE CODE	
17. SECURITY CLASSIFICATION OF REPORT	18. SECURITY CLASSIFICATION OF THIS PAGE	19. SECURITY CLASSIFICATION OF ABSTRACT	20. LIMITATION OF ABSTRACT
Unclassified	Unclassified	Unclassified	SAR

TABLE OF CONTENTS

	Page
1 INTRODUCTION	1
2 INTERACTION OF THE IMF AND THE EARTH'S MAGNETIC FIELD	2
3 DIGISONDE STATISTICAL DATA BASE	9
4 RESULTS FOR THE DETERMINATION OF BZ AND BY COMPONENTS.....	16
REFERENCES	23

LIST OF FIGURES

	Page
1 Artist view of Earth's magnetic fields and the Solar wind. Taken from Scientific America May 1989, page 58.....	3
2 Diagrams of the merging of the IMF and Earth's magnetic fields on the dayside, taken from Basinska 1992. a) When $Bz > 0$ the merging occurs at the poleward boundary [Russell, 1992]. b) When $Bz < 0$ merging occurs when the field lines are anti-parallel, at high latitudes on the dayside [Crooker, 1986].....	5
3 Idealized two-cell convection pattern set up when $IMF\ Bz < 0$	6
4 Idealized four-cell convection pattern set up when $IMF\ Bz > 0$	8
5 Polar E-field model results taken from Heppner Maynard [1987] showing the orientation of a two-cell system for different By signs. Also displays Digisonde drift results obtained from data recorded at Qaanaaq (Greenland) in 1989.....	10
6 Displays the orientation of a four cell system for different By values, taken from Kelley [1989] page 284.....	11
7 Top left displays averaged horizontal drift velocity component behavior for $Bz > 0$. Top right displays the horizontal drift velocity component measured on 10 Sept. 1990. Bottom graph displays the IMF results for 10 Sept. 1990.....	12
8 Shows the predicted azimuthal directions for the horizontal velocity components that should be observed at four high latitude stations when considering a simple two cell convection pattern.....	14

LIST OF FIGURES (continued)

Figure No.	Page
9 Shows Drift data measured at Qaanaaq (Greenland) from 9 to 11 April 1991.....	15
10 Displays a year of Qaanaaq drift data plotted for different Bz conditions. Only the azimuthal direction of the horizontal velocity component is plotted.....	17
11 Probability histograms for the direction of drift motion at Qaanaaq. 1989 data was used with velocities calculated from sources which had less than 10 degree phase error. All data independent of IMF.....	18
12 Comparison of the determined sign of the IMF Bz and By components using Digisonde velocity data, and IMF data recorded from the IMP-8 Satellite (Courtesy of R. Lepping GSFC).	20
13 Proportion of the percentage of correctly determined IMF Bz and By signs for 1989 data analyzed	21

LIST OF TABLES

Table 1. Drift Criteria for Different IMF Bz and By Orientations.....	19
---	----

1. INTRODUCTION

In recent years, a great deal of study has been devoted to the understanding of the interaction of the Interplanetary Magnetic Field (IMF) and the Earth's ionosphere. In trying to understand the electrodynamic system set up by the coupling of particles, fields and electric currents, several empirical and mathematical models have been developed to map out the convection patterns setup in the high latitude regions [Sojka et al 1986; Heppner and Maynard 1987; Hairston and Heelis, 1990]. In order to specify the convection pattern precisely these models require, as a minimum, inputs for the orientation of the IMF (sign of B_z and B_y components), and the position of the dayside cusp region and nighttime Harang discontinuity region. The essential advantage of these models lies in their ability to specify the real time convection pattern. In order to do this, real time data gathering of the required IMF and high latitude ionospheric responses is needed.

A network of ground-based observation stations (i.e. as is possible from the deployment of digital ionosondes), are capable of measuring and tracking rapid changes in the orientation of the IMF B_z and B_y components [Reinisch et al., 1987; Cannon et al. 1991] and the ionospheric behavior to these changes. Digital ionosondes are low maintenance, continuously operating instruments that simultaneously measure the electron densities and plasma velocities; the data can provide real time inputs for the specification of the convection models.

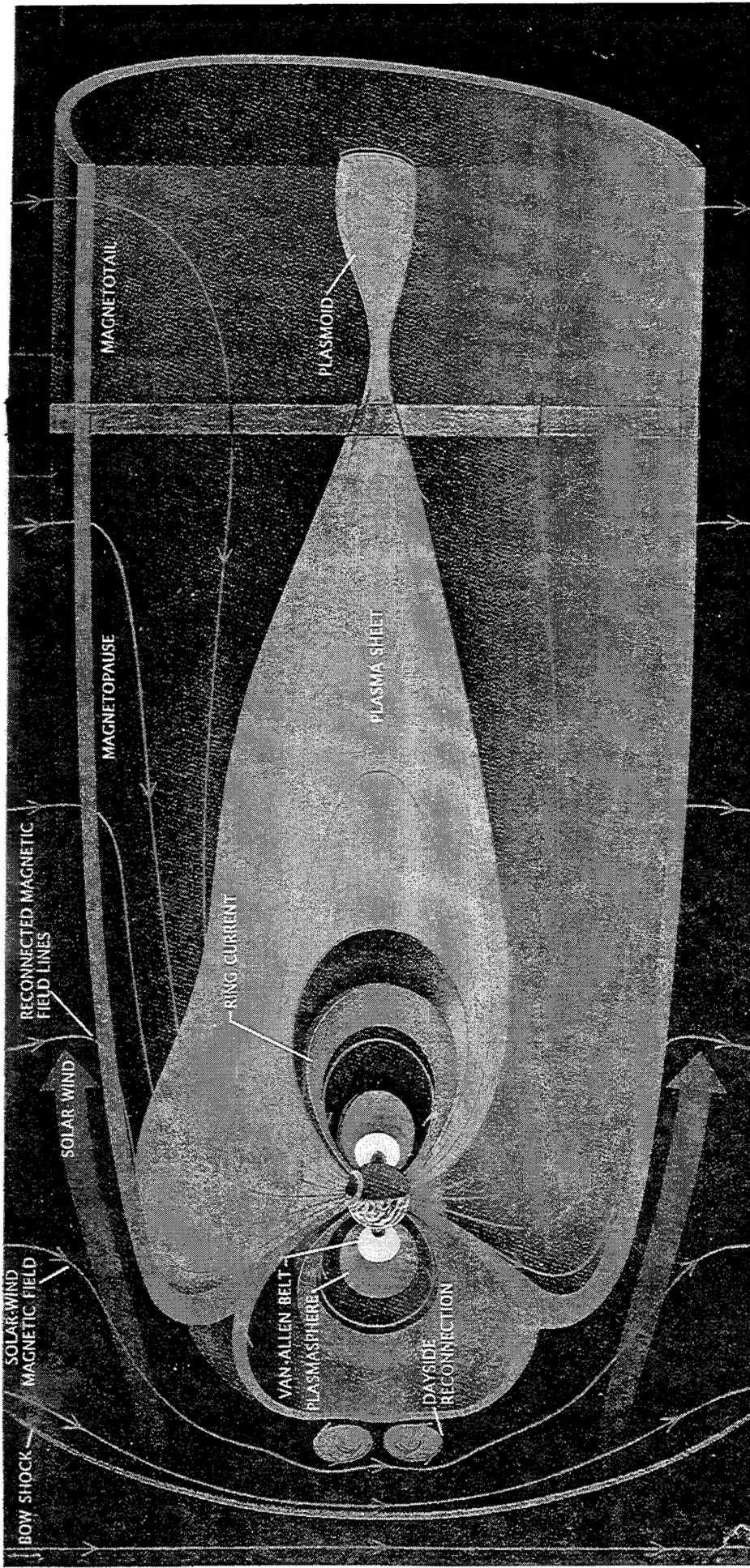
This report discusses the use of Digisonde drift velocities to determine the orientation of the IMF B_z and B_y components. Section 2 discusses the theory of the interaction of the IMF with the Earth's magnetic field, and the relations between the B_z and B_y orientations with convection patterns and velocity signatures observed by the Digisonde 256 system. Section 3 incorporates the statistical data base gathered by the Digisonde located at Qaanaaq and introduces criteria that help characterize the B_z and B_y orientations. Section 4 discusses the results of the analysis technique used to determine the B_z and B_y orientations and attempts to give an indication as to the reliability of these determinations.

2. INTERACTION OF THE IMF AND THE EARTH'S MAGNETIC FIELD

The interaction of the Earth's magnetic field with the IMF is observed in the magnetospheric-ionospheric system as the development of electrodynamic processes and the transfer of energy (via merging of field lines). An understanding of the dynamics involved is essential in order to better understand the effects that the B_z and B_y orientations have on high-latitude convection patterns. To a first order approximation, excluding the effect of the solar wind, the Earth's magnetic field can be considered to be a dipole in which the magnetic field lines loop from the south pole to the north pole. Including the solar wind this tends to confine the Earth's magnetic field to a comet-shaped volume as shown in Figure 1.

Since the charge in the solar wind experiences a force due to the Earth's magnetic field given as $F=qVxB$, these charges will be deflected around the earth. This has the effect of establishing secondary magnetic fields which cancel the earth's field on the sunward side and increase the value of the magnetic field on the nightside. The result, as observed in Figure 1, is to compress the magnetosphere to about $10R_E$ (where R_E = Earth radii) on the dayside, and elongate the magnetosphere to distances as much as $1000R_E$ on the nightside. In addition, the Earth slows down these charges from speeds as much as 400 km/s creating a bow shock (Figure 1).

Due to the "frozen-in" condition, the solar wind carries along with its plasma its own magnetic field. This magnetic field commonly referred to as the interplanetary magnetic field can interact with the Earth's magnetic field in two ways. On the dayside, dependent on the orientation of the B_z component, the solar wind magnetic field can "merge" with the Earth's magnetic field allowing the plasma to enter the Earth's magnetospheric environment, spiral along the magnetic field lines to the poles and be deposited at ionospheric heights. On the nightside, the solar wind may reconnect with the Earth's magnetic field similarly transferring energy. Magnetic field lines extending beyond the magnetosphere are called "open", while field lines extending to the boundary layer of inner magnetosphere are called closed. It is the establishment of electric fields along the opened and closed field lines that drive the convection pattern at high-latitudes.



lines in the north lobe of the magnetotail point toward the earth; those in the south point away. Reconnection of field lines in the magnetotail can pinch off clumps of plasma known as plasmoids, which are ejected from the magnetotail.

magnetotail, which extends for at least 1,000 earth radii. The boundary of the magnetotail is called the magnetopause. The solar wind has a magnetic field (red). When it is directed southward, as is shown here, it can "reconnect" efficiently with the earth's field (blue). Solar-wind particles flow into the magnetosphere along the reconnected field lines. Magnetic field

streaming from the sun, confines the earth's magnetic field in a comet-shaped cavity called the magnetosphere. The wind compresses the magnetosphere on the day side to a distance of about 10 earth radii. On the night side the wind sweeps the earth's magnetic field into an elongated volume known as the

Figure 1. Artist view of Earth's magnetic fields and the Solar wind. Taken from *Scientific America* May 1989, page 58.

Figure 2 shows how the IMF may merge with the Earth's magnetic field dependent on the orientation of B_z . Considering a Geocentric Solar Ecliptic coordinate system, for B_z southward ($B_z < 0$, Figure 2b), merging occurs at high latitudes [Crooker 1986]. For B_z northward ($B_z > 0$, Figure 2a) merging moves poleward of the dayside cusp [Russell, 1972]. Where the field lines merge is crucial in determining the convection pattern observed at high latitudes.

Consider the case for B_z southward first. The solar wind travels with velocity V_{sw} . In the case of the opened field lines, if B_{sw} is the magnetic field of the solar wind, then an electric field exists which in a reference frame fixed at the Earth is:

$$\mathbf{E}_{sw} = -\mathbf{V}_{sw} \times \mathbf{B}_{sw} \quad (1)$$

In the direction parallel to the Earth's magnetic field B , charged particles move freely. Hence, the Earth's magnetic field lines usually act like a perfect electrical conductor, transmitting perpendicular electric fields and voltages across vast distances with no change in the potential in the direction parallel to B . Thus, the electric potential established due to the IMF will apply across the magnetosphere and thus map down to ionospheric heights in the polar cap. This electric field will thus drive plasma in the F-region in the anti-sunward direction with a velocity given as:

$$\mathbf{V}_I = \frac{\mathbf{E}_I \times \mathbf{B}_I}{B_I^2} \quad (2)$$

Because the magnetic flux density is higher in the ionosphere than in the solar wind, and since the equipotential surfaces converge, the electric field in the ionosphere is larger than in the solar wind. The plasma in the polar ionosphere will therefore move in an anti-sunward direction (Figure 3) due to the mapping of the induced electric field produced from the merging of the solar wind magnetic field to the Earth's magnetic field.

Consider the electric field generation in the closed field line region of the magnetosphere. Due to the interaction of the solar wind, the Earth's magnetic field lines are distorted. The resulting magnetic geometry has a

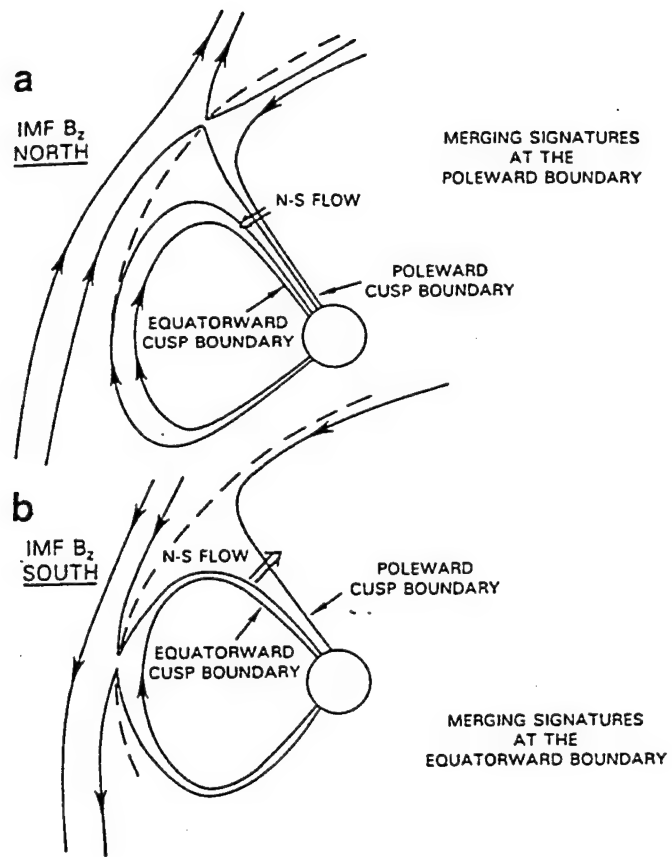


Figure 2. Diagrams of the merging of the IMF and Earth's magnetic fields on the dayside, taken from Basinska 1992. a) When $B_z > 0$ the merging occurs at the poleward boundary [Russell 1992]. b) When $B_z < 0$ merging occurs when the field lines are anti-parallel, at high latitudes on the dayside [Crooker 1986].

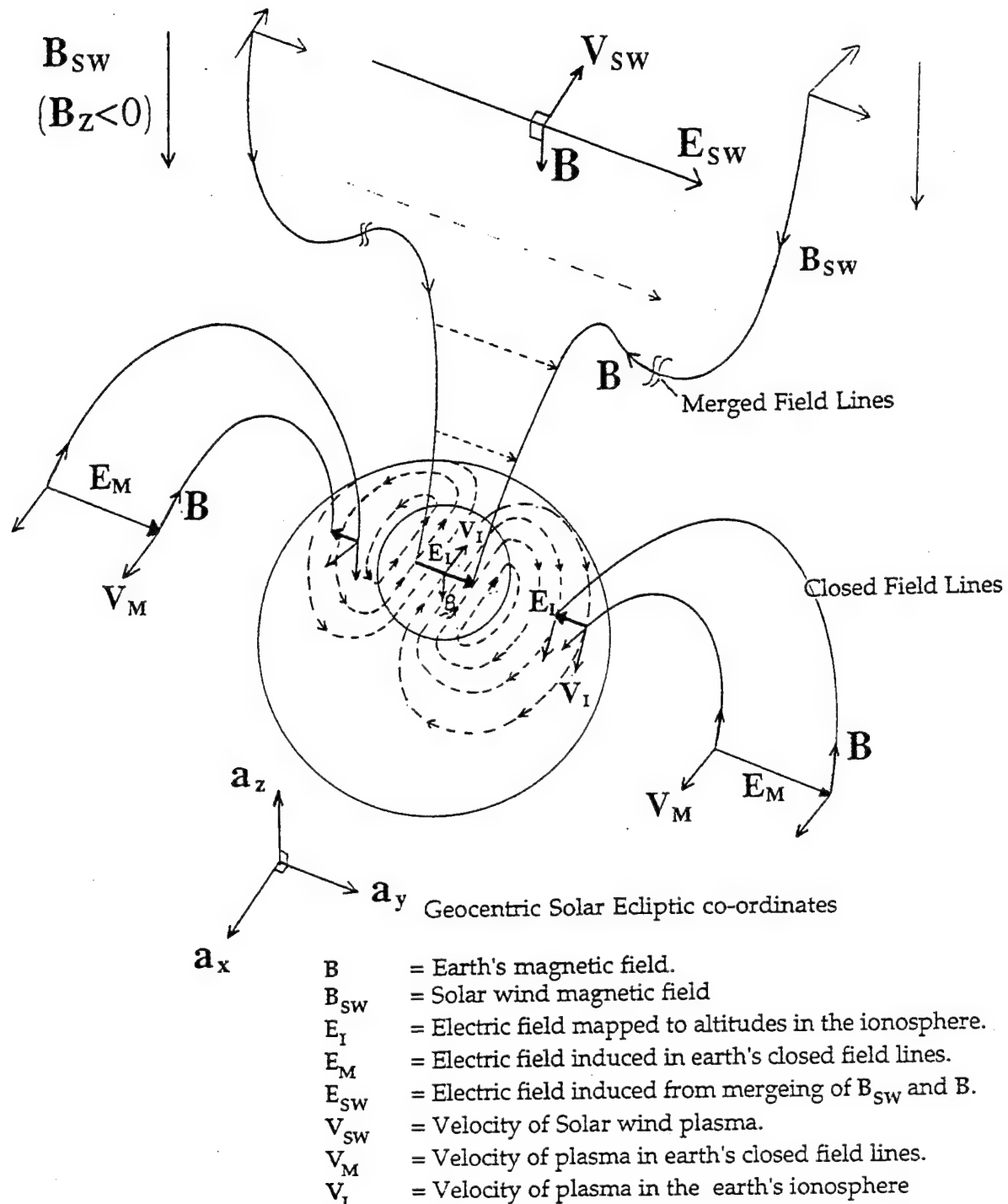


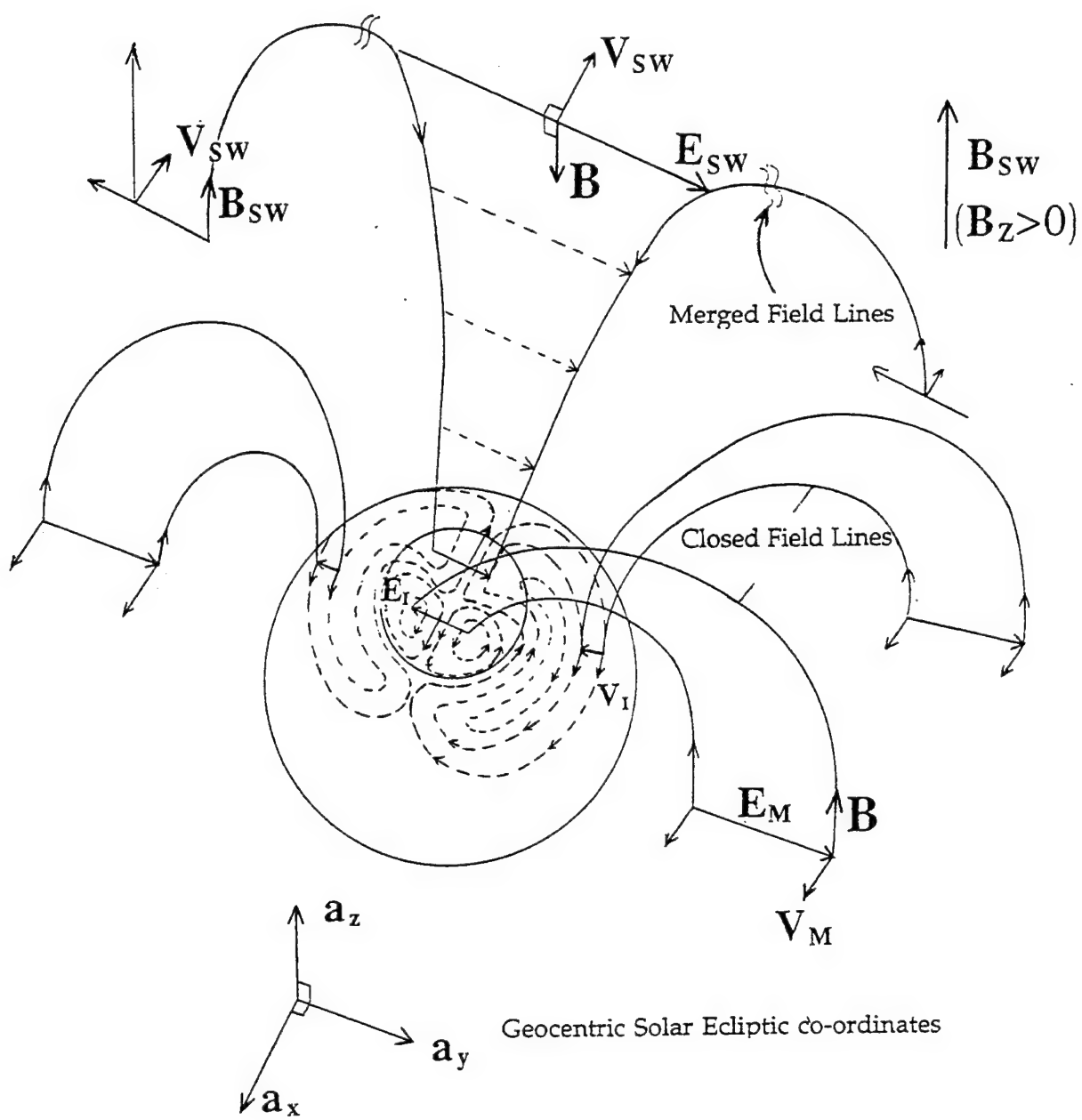
Figure 3. Idealized two cell convection pattern set up when $IMF\ Bz < 0$.

tension that exerts a force on the plasma. This together with the pressure gradient and the potential difference applied across the magnetosphere by the flowing solar wind, produce motion of the magnetospheric plasma on the closed field lines toward the sun. This motion induces a dawn to dusk electric field in the tail. Since this electric field is attributed to the flowing properties of the solar wind rather than its electro-magnetic properties, its dawn-to-dusk orientation will not be effected by the orientation of the B_z component.

In Figure 3, the electric field established in the magnetosphere due to the V_m motion of the plasma towards the sun is mapped to ionospheric heights. In the closed field environment, this electric field drives the plasma in the ionosphere sunwards establishing the outline of a two-cell motion. A great deal of literature exists discussing the two-cell motion described, so we will not devote any in-depth discussion of its characteristics at this stage but continue to the case when the IMF B_z component is pointed northward ($B_z > 0$).

In the case of the IMF B_z component being positive, a complete understanding of convection pattern and dynamics involved is still being developed. However, to a first approximation, we may use the discussions above to outline what convection pattern is possible. In the case of the open field lines, a B_z northward IMF component will induce a dusk-to-dawn electric field. When the IMF field lines merge with the Earth's magnetic field however, the induced electric field points from the dawn-to-dusk (Figure 4), as previously, and the plasma flows in an anti-sunward direction. Yet, as shown in Figure 2, the field lines merge poleward of the dayside cusp. This results in the field lines in the dayside polar region being closed.

For the case of the closed field lines as previously discussed, the magnetospheric electric field remains unchanged pointing from the dawn-to-dusk. Mapping of this electric field to lower latitudes drives the plasma sunward. Similarly, this field is also mapped to the dayside polar region and the addition of this sunward flow causes two smaller cells to develop. The two larger, lower latitude cells which would normally be observed for



$$B_I/B_{SW} = 50,000 \text{ nT}/5 \text{ nT} = 10^4$$

$$E_I/E_{SW} = 5 \text{ mVm}^{-1}/1 \text{ mVm}^{-1} = 50$$

$$V_I/V_{SW} = 1 \text{ kms}^{-1}/400 \text{ kms}^{-1} = 2.5 \times 10^{-3}$$

Figure 4. Idealized four cell convection pattern set up when IMF $B_z > 0$.

$B_z < 0$ and the two new smaller cells rotate in opposite directions. This "four" cell system has been observed experimentally; however, its characteristics are not as yet fully understood.

While the B_z component controls the location of the merging field lines and so determines the coarse structure of the convection pattern (two cell or four cell), the B_y component controls which field lines must contribute to the polar convection pattern. Hence, variations in B_y are outlined by the distortion of the two or four cell system. Figure 5 displays the orientation of modeled two cell convection patterns calculated by Heppner and Maynard [1987] for different B_y conditions. Also included are the Digisonde velocity measurements made at Qaanaaq, Greenland. This figure indicates that when $B_y < 0$ the dawn cell expands and the velocities in the polar region have directions slightly east of anti-sunward. When $B_y > 0$ the dusk cell dominates and velocities are directed west of anti-sunward direction. Both these features are clearly observable from the drift measurements made at Qaanaaq. Figure 6 displays the orientation of a four-cell system for different B_y values. (Taken from Kelley, 1989, p284). When B_y is small, the two smaller cells are symmetrical about the noon-midnight meridian. For $B_y < 0$ the dusk cell tends to expand into the dawn side and when $B_y > 0$ the reverse situation occurs.

3. DIGISONDE STATISTICAL DATA BASE

In order to determine B_z and B_y orientations it was necessary to interpret the velocities measured at a polar latitude station with known IMF orientations. An example of the Digisonde velocity data was already given in Figure 5. From data obtained from Qaanaaq over a three year period (1989-1991) estimates of the behavior of the motion of plasma due to different IMF conditions was possible. An example of how systematic the velocity pattern can be for certain IMF orientations is given in Figure 7 (Crowley et al., 1992). Figure 7 displays the polar plot for the average velocity behavior for $B_z > 0$ (top left plot). The velocity behavior measured on day 253 1990 is given on the right top plot along with the IMF B_x , B_y ,

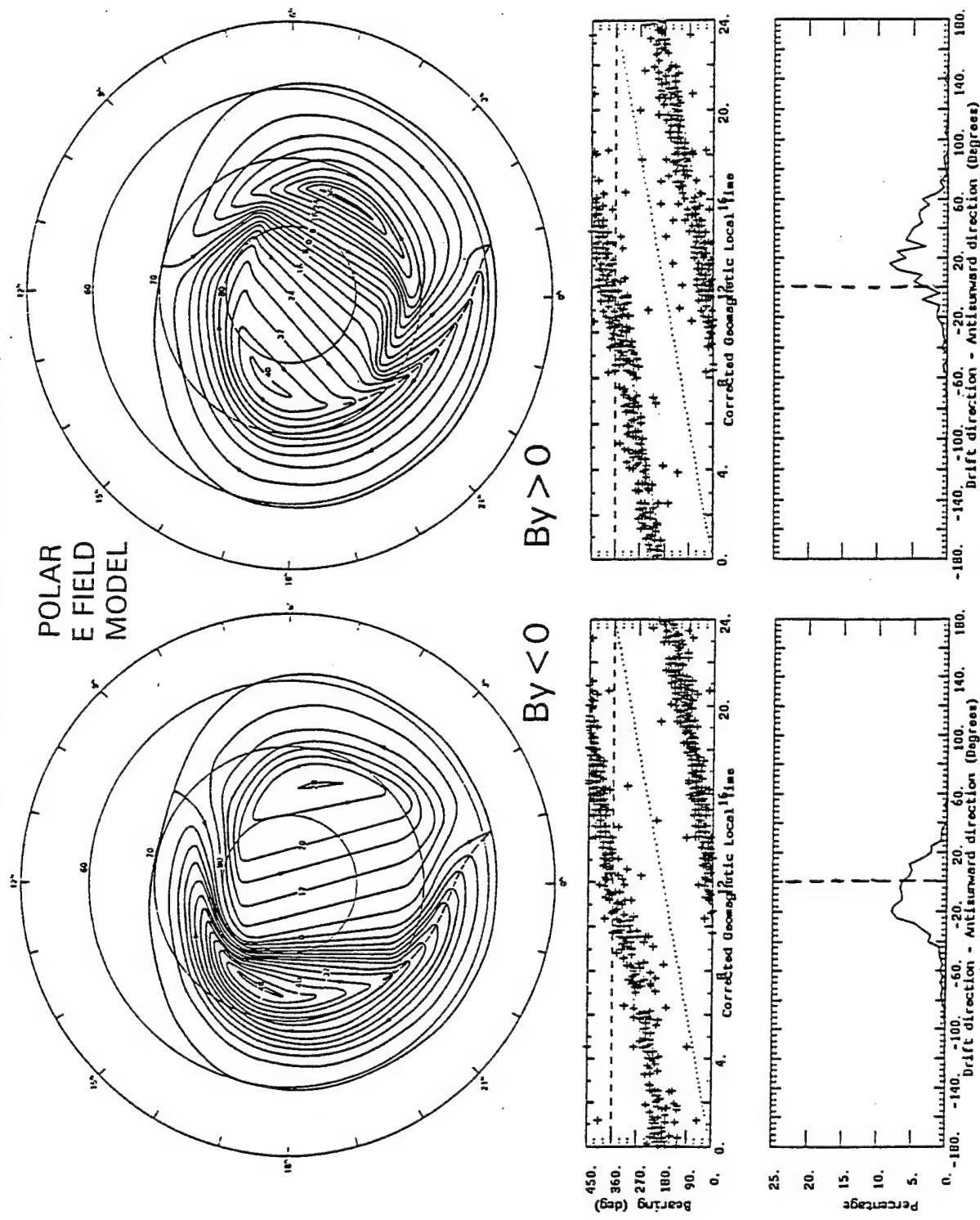
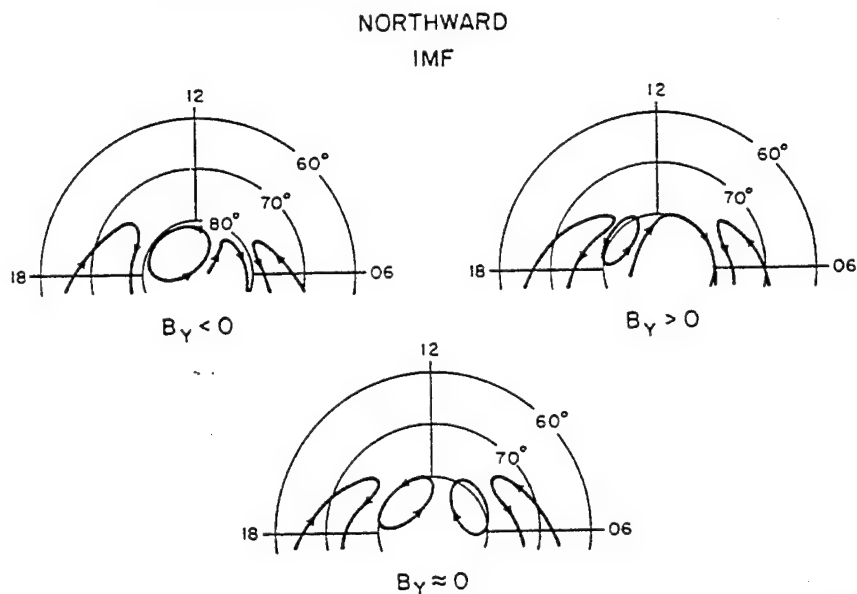


Figure 5. Polar E-field model results taken from Heppner Maynard [1987] showing the orientation of a two cell system for different B_y signs. Also displays Digisonde drift results obtained from data recorded at Qaanaaq (Greenland) in 1989.

6 High-Latitude Electrodynamics



The main feature of the dayside convection geometry when the IMF has a northward component is the existence of four convection cells. However, the dependence of the convection pattern on B_z leads to the dominance of one of the high-latitude cells and a three-celled pattern arises. [After Heelis *et al.* (1986). Reproduced with permission of the American Geophysical Union.]

Figure 6. Displays the orientation of a four cell system for different B_Y values, taken from Kelly [1989] page 284.

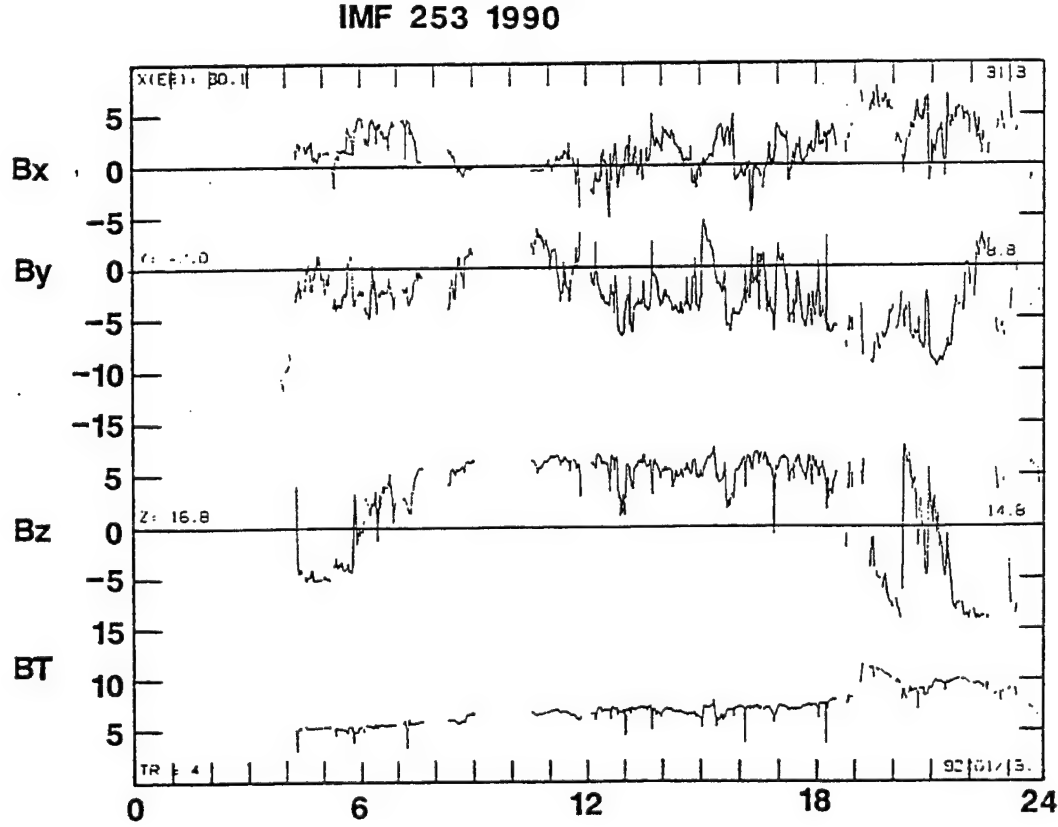
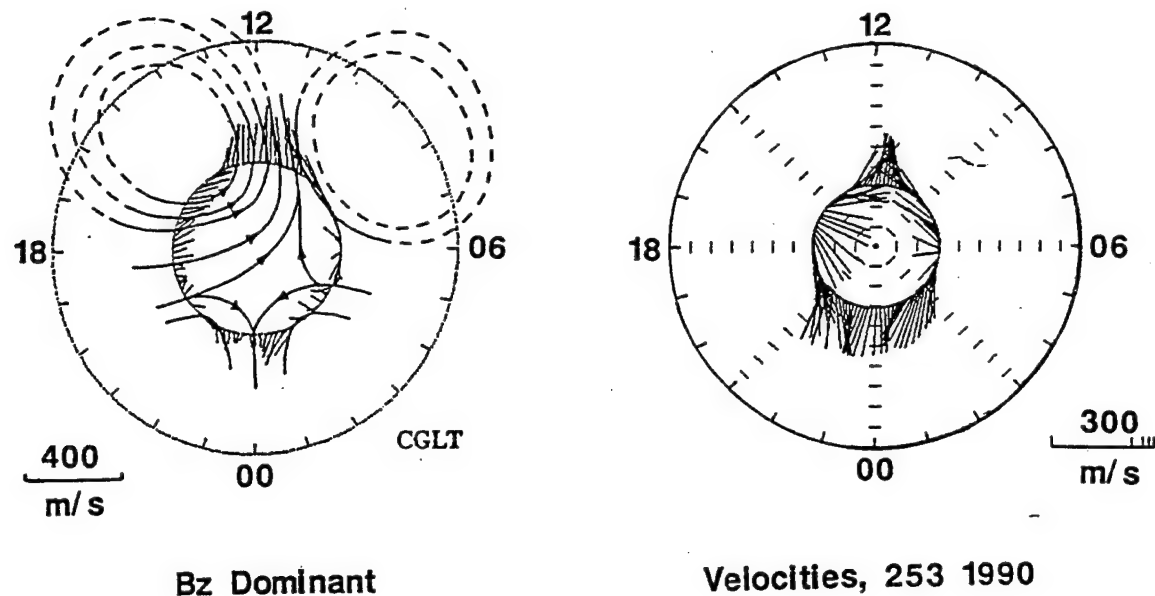


Figure 7. Top left displays averaged horizontal drift velocity component behavior for $B_z > 0$. Top right displays the horizontal drift velocity component measured on 10 Sept. 1990, Bottom graph displays the IMF results for 10 Sept. 1990.

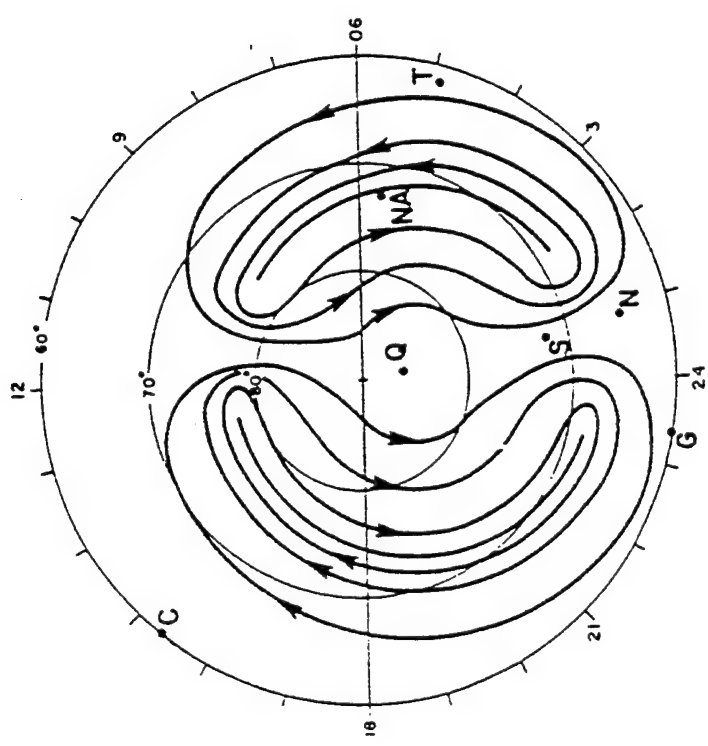
and B_z components measured for this day (bottom plot). Clearly, on day 253 1990 $B_z > 0$ and $B_y < 0$ for most of the day.

The velocities measured on this day show a similar pattern that is expected from the statistically averaged data. Hence, the top left plot is a good representation of velocity (convection) to expect when $B_z > 0$ and $B_y < 0$. Indeed one can characterize further comparisons such as these quickly and indicate what the B_z and B_y orientations are by just observing the drift velocities. Considering a simple two-cell convection pattern it is possible to outline the velocity behavior that should be observed at a number of latitudes. Figure 8 shows a simple two-cell pattern and the direction of the measured drift velocity that should be expected at four high-latitude stations.

The velocity plots are given as drift angle plotted as a function of time. For $B_z < 0$ at Qaanaaq the velocity component should be consistently anti-sunward. This is reflected in the linear graph for Qaanaaq as a gradual progression of the velocity direction from north through south to north in a 24-hour period. The signatures for the velocity directions expected at other stations reflect the stations location with respect to the convection cells.

Figure 9 shows drift data measured at Qaanaaq on days 99 to 101 1991. The horizontal velocity magnitude, vertical velocity and the azimuthal direction of the horizontal velocity are given in this plot. On day 99 the plasma flow is strictly anti-sunward. On day 100 after 12UT sunward motion is observed. We assume that at this time the B_z component reversed from southward to northward. Also, what is apparent is the lower horizontal velocity magnitudes when $B_z > 0$. These two distinct and simple characteristics of the behavior of the convection during changes in the IMF clearly indicate that the drift velocities may be used in the determination of the orientation of the IMF components.

Comparing known IMF orientations and velocity measurements made over one year, criteria were developed that relate variations in velocity to the signs of B_z and B_y . Figure 10 displays a year of Qaanaaq drift data plotted



POLAR DIGISONDE NETWORK AND THE CONVECTION PATTERN

°CG LATITUDE	STATION
87	QAANAAQ
75.5	NY ALESUND
75	SONDRE STROMFJORD
69	NARSSARSSUAQ
66	TROMSO
65	COLLEGE
65	GOOSE BAY
58	ARGENTIA

PREDICTED NOMINAL PLASMA FLOW PATTERNS FOR $B_Z < 0$

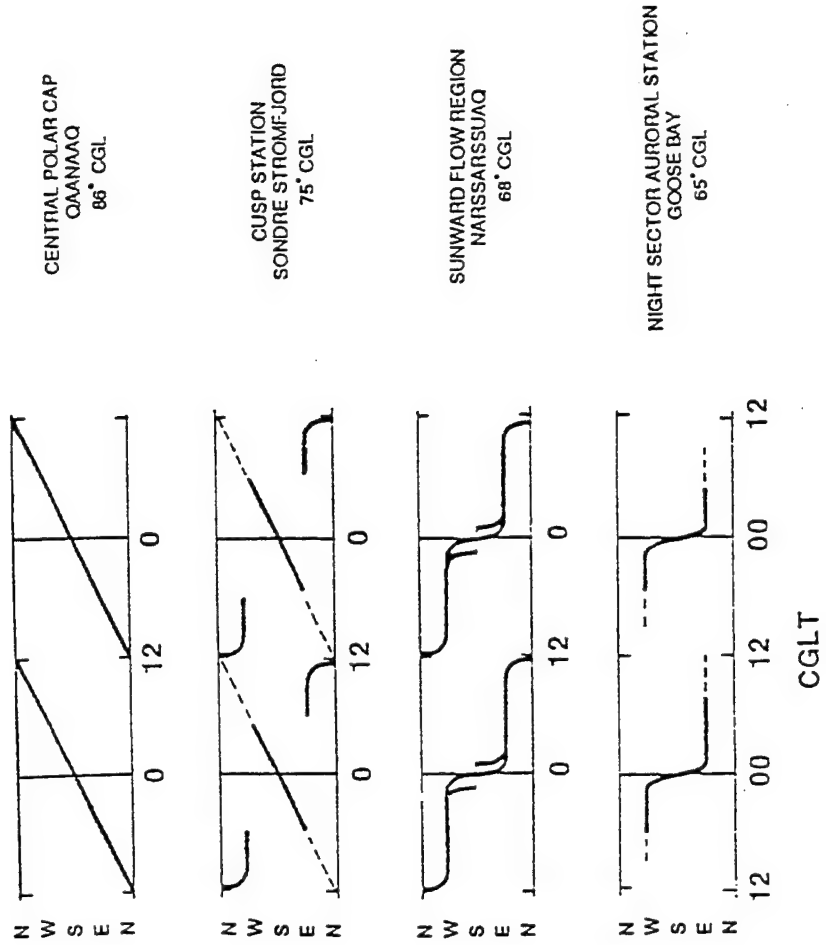


Figure 8. Shows the predicted Azimuthal directions for the horizontal velocity components that should be observed at four high latitude stations when considering a simple two cell convection pattern.

Drift Velocities recorded at Qaanaaq (Greenland)

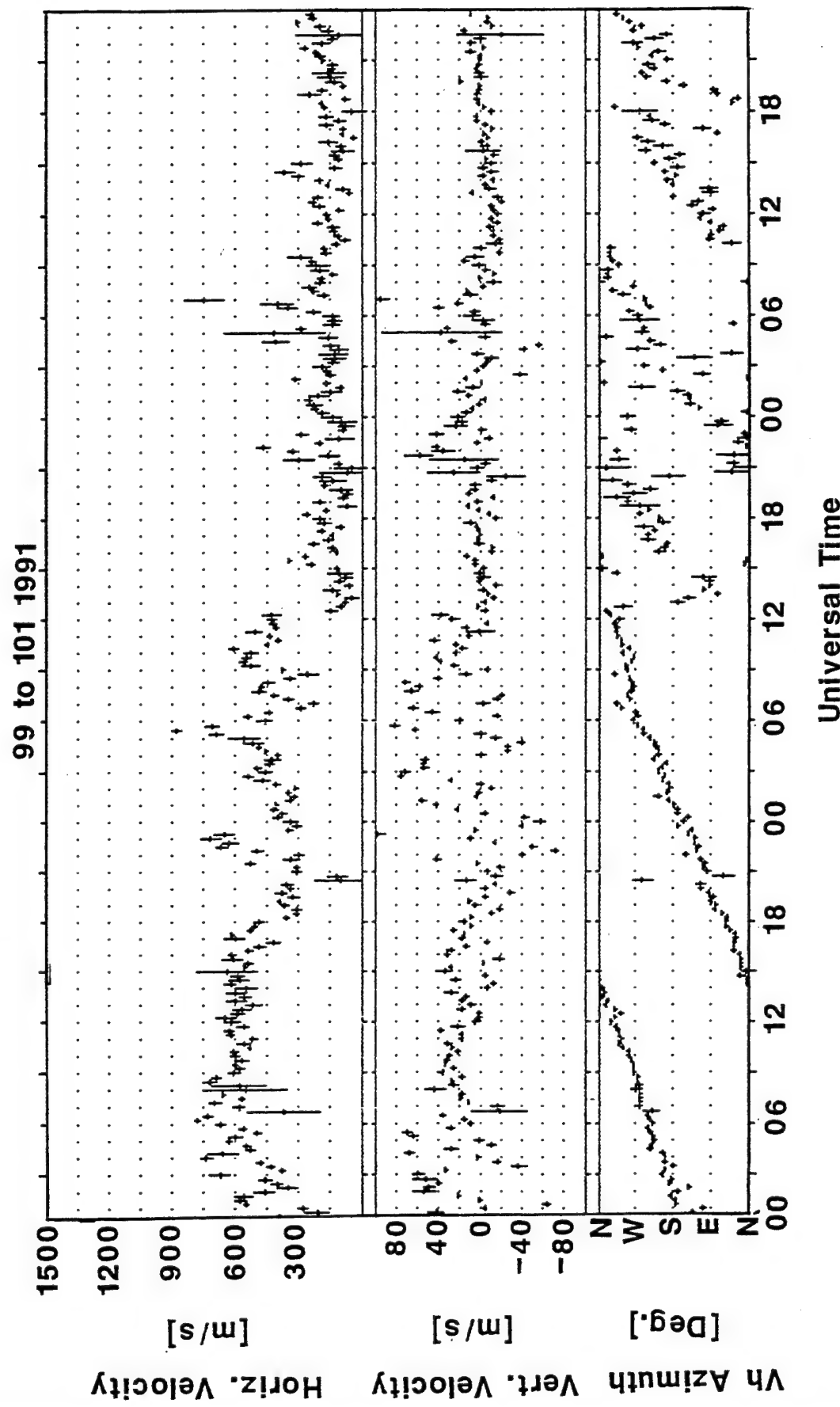


Figure 9. Shows Drift data measured at Qaanaaq (Greenland) from 9 to 11 April 1991.

for different B_z conditions. What is clear from this figure is the existence of a sunward drift observed during 08 to 18CGLT for $B_z > 0$ which is nonexistent for $B_z < 0$. From the discussions in Section 1 this is not surprising. The sunward flow of plasma around 12CGLT for $B_z > 0$ correlates well with the development of the four cell system. In this Figure alone, a criteria exists that if sunward motion is observed between 08 and 18CGLT, B_z is definitely positive.

The extent and intensity of the spread observed in the scatter plots shown in Figure 10, indicates that distribution limits could be imposed on this data in order to test if a velocity component belongs to $B_z < 0$ or $B_z > 0$ condition. Figure 11 shows a set of horizontal drift velocity distributions produced for 3 hour periods. The movement of the mean of these distributions from -180 to 180 degrees outlines the anti-sunward motion observed in Figure 10. Each distribution has a finite width represented by a standard deviation of 20 degrees. Testing a horizontal velocity azimuth against any one of these distributions would indicate if the velocity measured is anti-sunward or sunward. Developing such tests would, in turn, allow us to interpret the orientation of the IMF components. For example, 12CGLT at Qaanaaq a horizontal velocity azimuth of 160 degrees was measured. From the statistical distribution given for 1030 to 1330CGLT the anti-sunward motion has a mean at 10 degree and a standard deviation of 20 degrees. The measured velocity must clearly be classified as sunward, not anti-sunward and with reference to Figure 10 one can immediately conclude that the B_z component is positive.

In developing a statistical testing package, a list of criteria for different IMF B_z and B_y orientations was established which is summarized in Table 1. One important feature is that the larger velocities are always associated with $B_z < 0$, and that for $B_z > 0$ no substantial separation in the velocities is noticeable.

4. RESULTS FOR THE DETERMINATION OF B_z AND B_y COMPONENTS

Using the criteria above and allocating confidence weights for the one, two

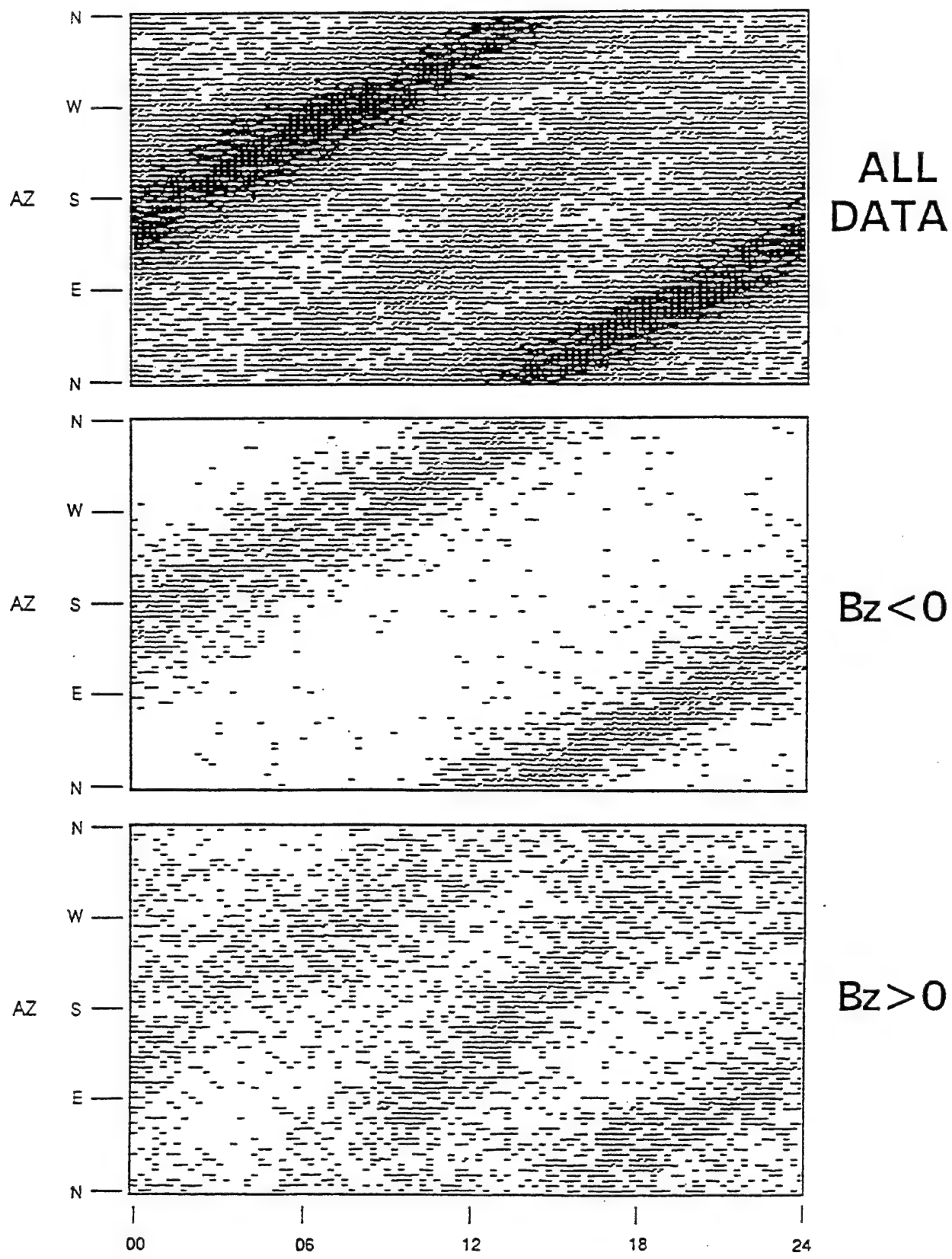


Figure 10 Displays a year of Qaanaaq drift data plotted for different B_z conditions. Only the azimuthal direction of the horizontal velocity component is plotted.

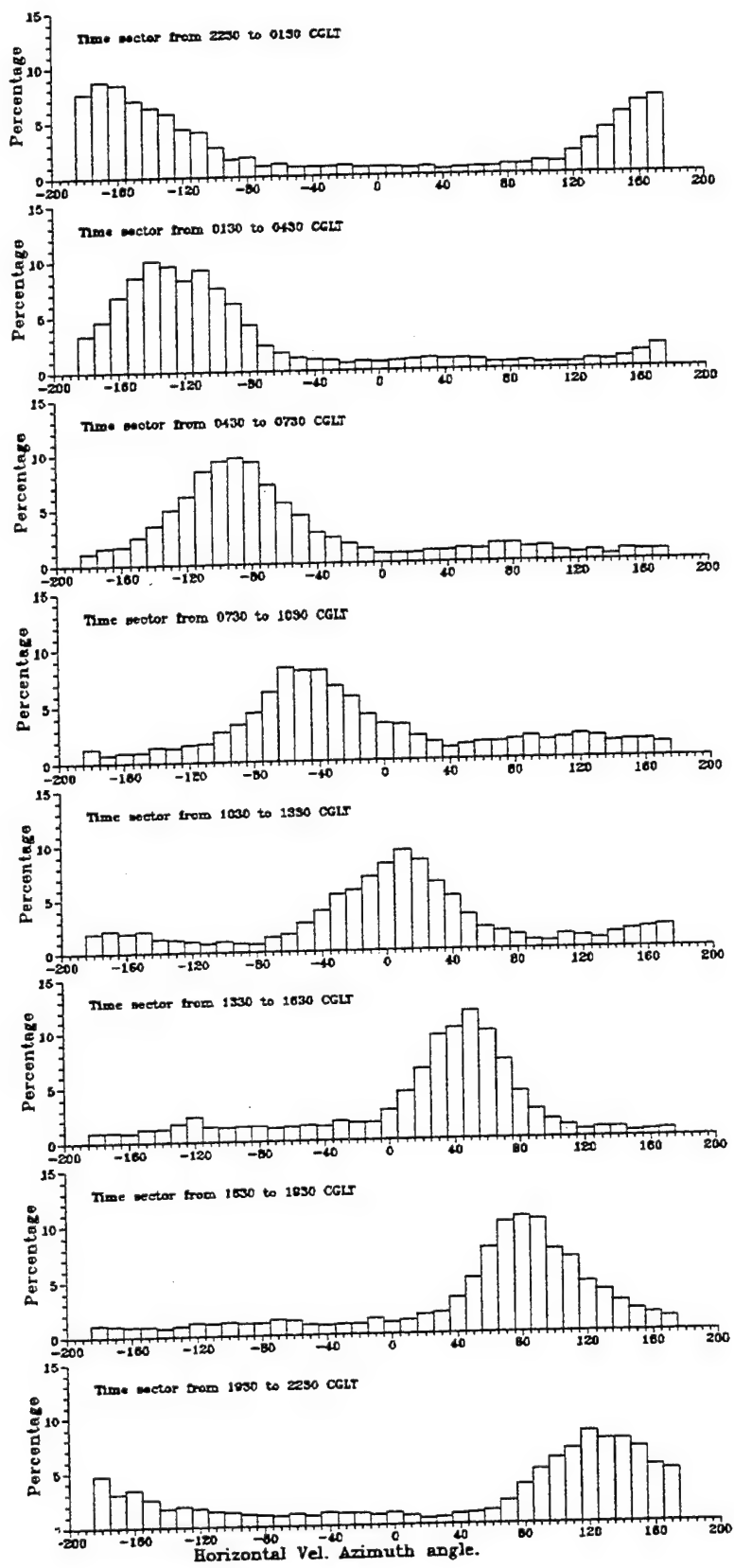


Figure 11 Probability histograms for the direction of drift motion at Qaanaaq. 1989 data was used with velocities calculated from sources which had less than 10 degree phase error. All data independent of IMF. Azimuth angle is measured from north.

Table 1. Drift Criteria for Different IMF Bz and By Orientations

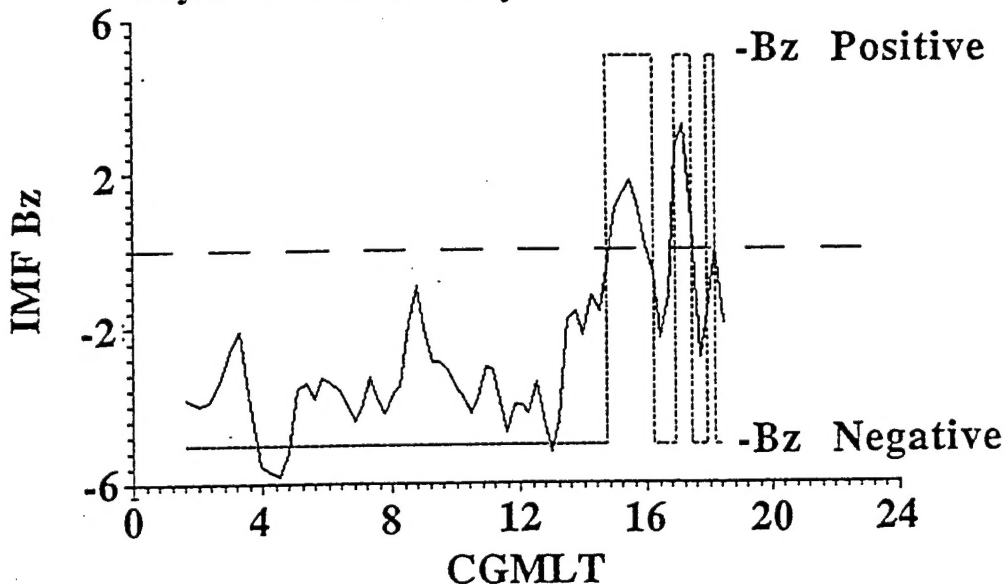
IMF	Deviation (degree) Drift-Anti-sunward		Horizontal Magnitude m / s		Time Int. (CGLT)
	Mean	S.D.	Mean	S.D.	
Bz \leq 0	0	20	≥ 600	100	ALL
By \leq 0	$\Delta 0$	60	≤ 200	100	01 to 12
By \leq 0	$\Delta 0$	60	≥ 600	100	13 to 24
By $>$ 0	$\Delta 0$	60	≥ 600	100	01 to 12
By $>$ 0	$\Delta 0$	60	≤ 200	100	13 to 24
Bz $>$ 0	180	20	< 300	100	
By \leq 0	$\Delta 0$	60	≤ 200	100	18 to 06
By \leq 0	> -180	60	≤ 200	100	07 to 17
By $>$ 0	$\Delta 0$	60	≤ 200	100	18 to 06
By $>$ 0	< 180	60	≤ 200	100	07 to 17

and three standard deviation it is possible to determine the sign of the IMF Bz and By components from the Digisonde velocity measurements. Dependent on which increment the velocity value was located would indicate how confident the determined Bz and By orientation was. Figure 12 displays a comparison of determined Bz and By orientations and actual measured IMF values recorded for 1 January 1989. The continuous line displays the satellite measured IMF value while the dashed line gives the sign of the IMF value determined from the Digisonde velocities. The overall comparison is good; the percentages of times Bz and By were determined correctly were 95.4 and 81.6 respectively. In this example, some inconsistencies in the determination of the sign of the IMF By component can be seen.

Testing this method with one year worth of drift data recorded at Qaanaaq, it is possible to determine the correct IMF Bz and By orientations 60-70% of the time. Figure 13 shows the percentage distributions for the determination of Bz and By from the 1989 drift data collected at Qaanaaq.

Keeping in mind that all CGL times are tested, and only a single velocity measurement is used at any one time to determine the Bz and By components, this result is surprisingly good.

Determination of IMF Bz Sign from Digisonde Drift
 Continuous Line = Averaged IMF Bz (IMP8) Data
 Dashed Line = Determined IMF Bz Sign
 Percentage correctly determined = 95.4
 Day/Year : 1 January 1989



Determination of IMF By Sign from Digisonde Drift
 Continuous Line = Averaged IMF By (IMP8) Data
 Dashed Line = Determined IMF By Sign
 Percentage correctly determined = 81.6
 Day/Year : 1 January 1989

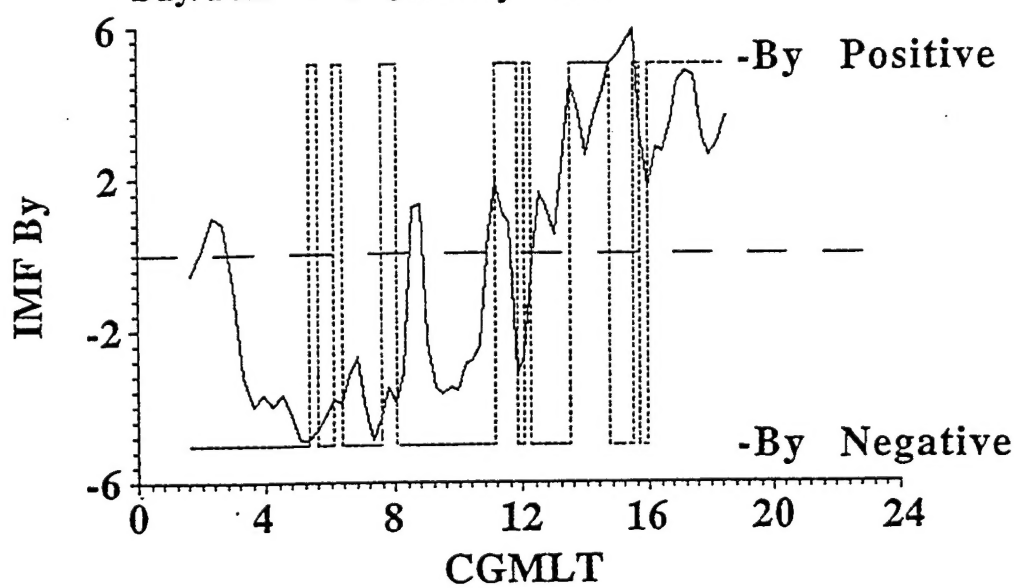


Figure 12. Comparison of the determined sign of the IMF Bz and By components using Digisonde velocity data, and IMF data recorded from the IMP-8 Satellite (Courtesy of R. Lepping GSFC).

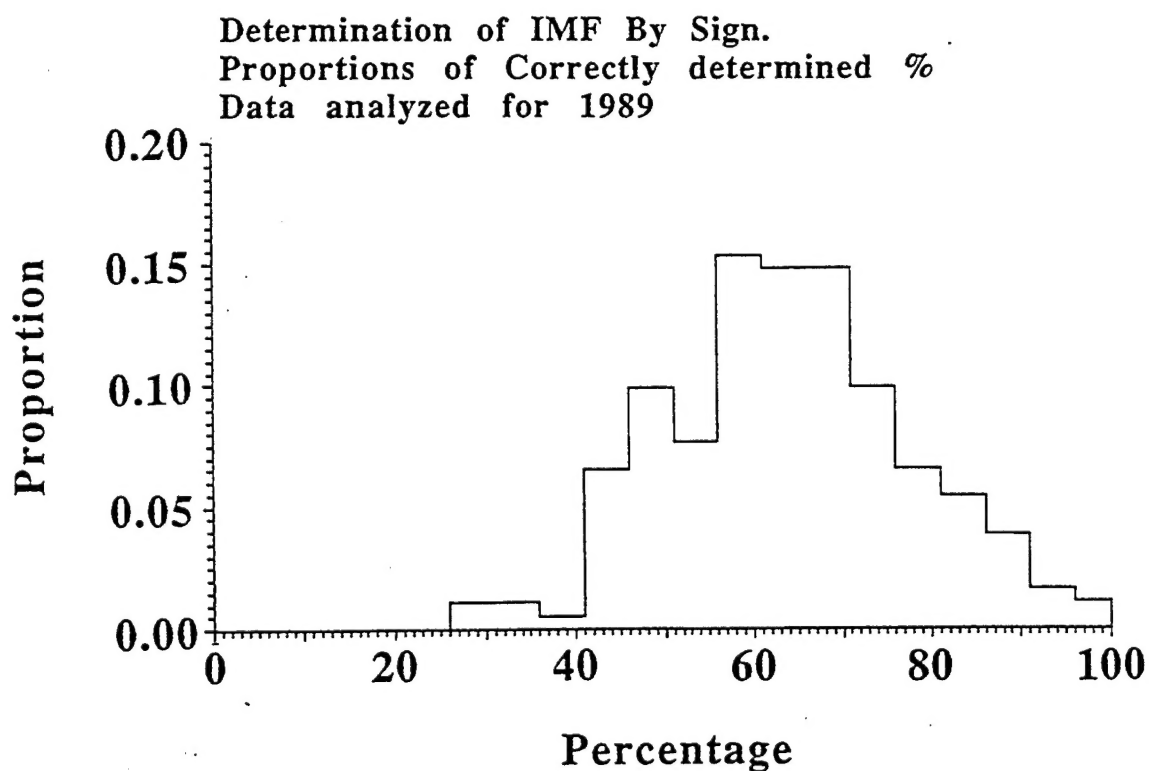
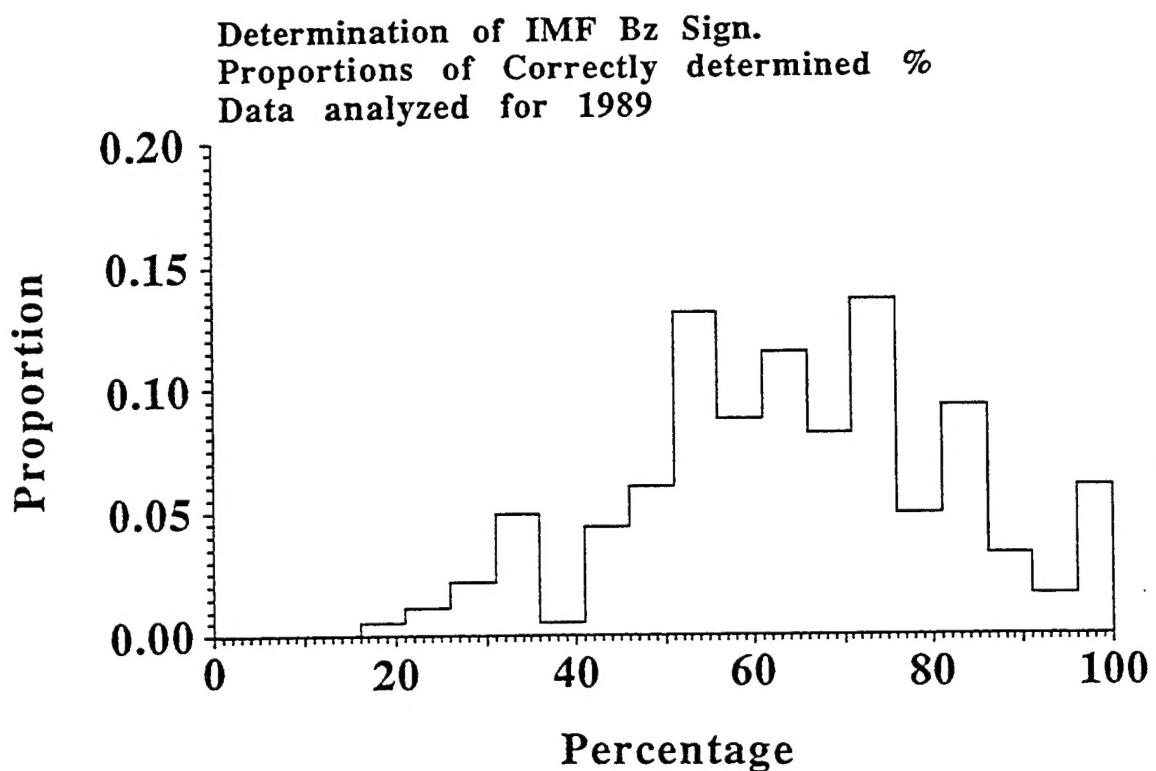


Figure 13. Proportion of the percentage of correctly determined IMF Bz and By signs for 1989 data analyzed.

The method which bases its results on a single station and only one velocity measurement, still requires additional work in order to improve on the determination of IMF Bz and By components. The areas that still need to be addressed are:

1. Introduce a time history into the analysis to indicate if an individual determined IMF orientation is consistent with previous measurements, or if the IMF Bz and By signs have changed.
2. Due to overlapping of similar velocities for certain time periods these methods should only be tested when the stations are in those CGLT sectors where the convection patterns are clearly defined for different Bz and By orientations. As an example, at Qaanaaq Bz may be unambiguously determined during the time interval from 09 to 15 CGLT when $Bz < 0$ produces anti-sunward flow and while $Bz > 0$ produces sunward flow. However, from 09 to 15 CGLT anti-sunward convection is observed for both $Bz > 0$ and $Bz < 0$. Hence, for Qaanaaq it would be best to rely only on the determined values when the station is located in the 09 to 15 CGLT sector (see item 4 below).
3. Improve the velocity calculation in the presence of velocity shears in the field-of-view of the sounder.
4. Use other high latitude stations to cover all time periods and several latitudes to establish a more robust prediction capability for the Bz and By directions.

ACKNOWLEDGEMENT

The authors wish to acknowledge the encouragement and guidance provided by Phillips Laboratory's Jurgen Buchau until his death on 9 August 1993, and by Terence Bullett.

REFERENCES

Basinska, E.M., W.J. Burke, N.C. Maynard, W.J. Hughes, J.D. Winningham, and W.B. Hanson, "Small-Scale Electrodynamics of the Cusp with Northward Interplanetary Magnetic Field", *J.G.R.*, Vol. 97 pp 6369-6379, 1992.

Cannon, P.S., B.W. Reinisch, J. Buchau and T.W. Bullett, "Response of the Polar Cap F Region Convection Direction to Changes in the Interplanetary Magnetic Field: Digisonde Measurements in Northern Greenland," *J. Geophys. Res.*, 96, A2, pp. 1239-1250, 1991.

Crowley, G., P.S. Cannon, C.G. Dozois, B.W. Reinisch, and J. Buchau, "Polar Cap Convection for Bz Northward," *Geophys. Res. Ltrs.*, 19, No. 7, pp. 657-660, 1992.

Crooker, N.U., "An Evolution of Antiparallel Merging," *Geophys. Res. Ltrs.*, 13, pp. 1063-1066, 1986.

Hairston, M.R. and R.A. Heelis, "Model of the High-latitude Ionospheric Convection Pattern During Southward Interplanetary Magnetic Field Using DE-2 Data," *J. Geophys. Res.*, Vol. 95, pp 2000-2343, 1990.

Heppner, J.P. and N.C. Maynard, "Empirical Models of High Latitude Electric Field Models," *J. Geophys. Res.*, Vol. 92, pp 4467-4489, 1987.

Kelley, M.C. "The Earth's Ionosphere," Academic Press, Inc., 1989.

Reinisch, B.W., J. Buchau and E.J. Weber, "Digital Ionosonde Observations of the Polar Cap F Region Convection," *Physica Scripta*, 36, pp. 372-377, 1987.

Russell, C.T., "The Configuration of the Magnetosphere, in Critical Problems of Magnetospheric Physics," edited by E.R. Dryer, Inter-Union Common on Solar-Terrestrial Physics, National Academy of Sciences, Washington, D.C., 1972.

Sojka, J.J., C.E. Rasmussen and R.W. Schunk, "An Interplanetary Magnetic Field Dependent Model of the Ionospheric Convection Electric Field," *J. Geophys. Res.*, Vol. 91, pp 11281-11290, 1986.